International Journal of Engineering Research & Technology (IJERT)
ISSN: 2278-0181
Vol. 15 Issue 11 , November - 2026

Conversion of a High-Speed Passenger Boat into an Aerodynamically Alleviated Marine Vehicle for Improved Performance using an Optimization Method.

[1]Owoidoho I. Brown; [2]Ephraim R. Afia; [3]Joy E. Edet; [4]Anietie E. Udo

[1,3] Department of Naval Architecture, Federal University of Technology, Ikot Abasi (FUTIA), Akwa Ibom State, Nigeria.

[2] Department of Mechanical Engineering, Federal University of Technology, Ikot Abasi (FUTIA), Akwa Ibom State, Nigeria.

[4] Department of Marine Engineering/ Naval Architecture, Akwa Ibom State University, Ikot Akpaden (AKSU), Akwa Ibom State, Nigeria.

Abstract - High-speed marine vehicles (HSMVs) used for passenger transport in Nigerian coastal waters operate with high hydrodynamic resistance and power demand. This study develops and applies a numerical procedure for converting an existing high-speed passenger boat into an aerodynamically alleviated marine vehicle (AAMV) by fitting an aerodynamic lifting surface (wing) to the hull. The computational fluid dynamics (CFD) model, based on the Reynolds-averaged Navier–Stokes equations with the volume of fluid method, was first checked against two published planing hull cases. A model-scale hull of an existing passenger boat operating in Ikot Abasi, Nigeria, was then simulated with and without the wing at a speed of 7.1 m/s. The position of the wing was optimized with a screening multi-objective direct optimization method in ANSYS, using ten design points generated within prescribed bounds of the longitudinal, transverse and vertical (X, Y, Z) wing coordinates. The resistance of the boat without the wing was 1809 N. Fitting the wing at the reference location reduced it to 1769.5 N (2.2%), and at the optimal location (X = -0.3 m, Y = 0.07 m, Z = -0.419 m) the hydrodynamic resistance fell to 1689 N, a reduction of 6.6%, with a hydrodynamic lift of 2454.6 N, a wing drag of 9.25 N and a wing lift of 3.58 N. Including the wing drag, the total resistance and the effective power at the design speed were reduced by about 6.1%. The study provides a practical, simulation-based procedure for converting existing high-speed passenger boats into AAMVs with improved hydrodynamic performance.

Keywords: Aerodynamically Alleviated Marine Vehicle, High-Speed Passenger Boat, Planing Hull, Computational Fluid Dynamics, Multi-Objective Optimization, Resistance Reduction

1.0 INTRODUCTION

The demand for faster, safer, more economical and more comfortable sea transport has driven the development of high-speed marine vehicles (HSMVs) (Faltinsen, 2006). Conventional displacement hulls experience a steep rise in wave-making resistance as speed increases, which has led designers to adopt alternative lifting mechanisms and hull forms, including planing hulls, hydrofoils, multihulls, air-cushion craft and hybrid configurations (Collu et al., 2009). These developments gave rise to modern HSMVs and to aerodynamically alleviated marine vehicles (AAMVs). In HSMVs, hydrodynamic pressure on the hull bottom generates lift that, as speed increases, reduces the wetted surface and changes the running trim (Faltinsen, 2006). Nevertheless, resistance, power demand, dynamic motion and fuel consumption remain important performance considerations for HSMVs (Tavakoli et al., 2024). Multihulls such as catamarans and trimarans were introduced to provide a larger deck area, greater transverse stability and lower wave-making resistance, although they may suffer from structural, trim, pitching or wave-induced motion problems (Faltinsen, 2006). In practice, planing monohulls, catamarans and hydrofoil-assisted catamarans have become common, and studies have shown how hull shape and hydrodynamic features affect their resistance and dynamic performance (Giraldo-Pérez et al., 2022; Ohwofadjeke et al., 2024). Hydrofoils generate hydrodynamic lift through submerged foils, which reduces the immersion and wetted area of the hull and can improve stability, although cavitation, ventilation,

(This work is licensed under a Creative Commons Attribution 4.0 International License.)

International Journal of Engineering Research & Technology (IJERT)
ISSN: 2278-0181
Vol. 15 Issue 11 , November - 2026

structural loads and stability remain important design considerations (Faltinsen, 2006). These advances have led to hybrid concepts such as the AAMV, which is supported by both hydrodynamic and aerodynamic forces. By transferring part of the lift from the water to the air, an AAMV reduces the hydrodynamic lift required from the hull and, with it, the hydrodynamic drag (Collu et al., 2009; James & Collu, 2015). CFD analyses have shown that the losses of ultra-high-speed AAMVs can be reduced when aerodynamic lift becomes the dominant component of the total lift (Ni et al., 2023). Further studies have examined AAMV resistance and motion in regular waves (Song et al., 2023) and AAMV stability in wind and waves, showing that the design parameters and the relative positions of the center of gravity and the aerodynamic center of pressure govern longitudinal stability (Song, Du, & Hu, 2024). Low resistance at high speed is a key requirement for marine vehicles. Over many years, four sustaining forces, namely hydrostatic (buoyancy), powered aerostatic, hydrodynamic and aerodynamic forces, have been combined to produce a range of faster marine vehicle types (James & Collu, 2015). Together these forces form the lift pyramid shown in Figure 1, which covers most existing marine vehicles. The region of Figure 1 in which the weight is supported by a combination of buoyancy, hydrodynamic lift and aerodynamic lift is the Aerodynamic Alleviation Zone (AAZ), and the vehicles in this zone are AAMVs (Collu et al., 2009).

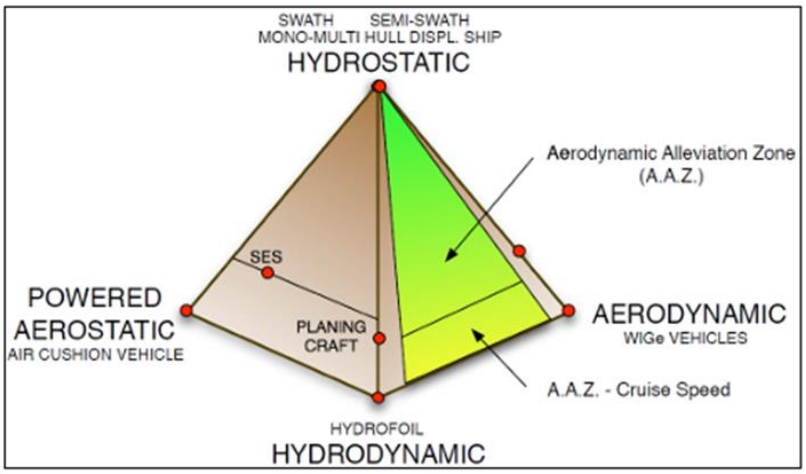

Figure 1: Classification of marine vehicles based on their sustaining (lift) forces (Collu et al., 2009)

Although the AAMV concept has reached a degree of maturity, many existing HSMVs in Nigerian waters, for example in Ikot Abasi Local Government Area alone, operate under demanding operational requirements. This study therefore seeks to demonstrate the benefit of converting such craft into AAMVs by adding an aerodynamic feature, namely a wing.

As operating speed increases, high-speed boats experience growing hydrodynamic resistance, changes in hydrodynamic lift and trim, wetted-surface effects and wave-making. Although hydrodynamic lift allows HSMVs to reach high speeds, sustaining it requires considerable propulsion power, which increases fuel consumption (Faltinsen, 2006; Tavakoli et al., 2024). Constraints on hull geometry, draft, structural arrangement, passenger capacity and propulsion systems further complicate efforts to improve the performance of existing high-speed boats (Samaei & Asadian, 2025; Yun et al., 2018). Conventional approaches based on hull modification, propulsion improvement or additional hydrodynamic lifting devices may therefore be of limited use, and they can introduce additional resistance or motion problems, as observed with hydrofoils. An alternative is to apply AAMV features, which combine hydrodynamic and aerodynamic lift. Aerodynamic surfaces have been shown to provide significant lift that affects both the resistance and the longitudinal stability of HSMVs (Ni et al., 2023; Song, Du, & Hu, 2024). However, existing studies have focused mainly on ultra-high-speed, purpose-built or conceptual AAMVs, and very few have addressed the systematic conversion and optimization of existing high-speed passenger boats. This is the principal

(This work is licensed under a Creative Commons Attribution 4.0 International License.)

International Journal of Engineering Research & Technology (IJERT)
ISSN: 2278-0181
Vol. 15 Issue 11 , November - 2026

research gap addressed in this study. Moreover, because the aerodynamic and hydrodynamic forces are coupled, drag, lift, trim, pitch, heave and longitudinal stability all change with the geometry, position and incidence of the aerodynamic surface. Studies of AAMV behavior in wind and waves show that the suitability of an AAMV configuration cannot be judged on resistance reduction alone (Song, Du, & Hu, 2024; Song et al., 2023). A systematic procedure is therefore needed to assess the baseline performance of a given HSMV, such as a passenger speed boat, apply suitable aerodynamic modifications, model the resulting aero-hydrodynamic changes and optimize the relevant design parameters while maintaining acceptable performance. To this end, the present study combines CFD modeling with optimization and compares the aerodynamically modified boat with the conventional HSMV. The aim is to analyze the conversion of a standard high-speed passenger boat into an aerodynamically optimized passenger boat.

Several numerical studies of AAMVs have been reported. Song et al. (2023) investigated the aerodynamic and hydrodynamic characteristics of an ultra-high-speed AAMV and showed that aerodynamic lift becomes an increasingly important part of the total lift at high speeds. Ni et al. (2023) applied finite-volume CFD to the same class of vehicle and assessed how different hull and wing configurations influence its resistance. Their results highlight the importance of treating the aerodynamic surfaces and the hull as a coupled system rather than as two separate components. Aerodynamic surfaces generate lift and drag as well as pitching moments about the center of gravity (Matveev & Dubrovsky, 2007), so their geometry, position, area and orientation affect not only resistance but also trim and longitudinal stability. Collu et al. (2009) developed a mathematical framework for designing HSMVs with aerodynamic surfaces, and Collu et al. (2010) examined the longitudinal static stability of AAMVs, highlighting the importance of the relative positions of the aerodynamic center and the center of gravity. This interaction makes AAMV design fundamentally different from simply adding a wing to a conventional boat. The aerodynamic and hydrodynamic systems must be treated as an integrated configuration. Waves and environmental disturbances also affect AAMV behavior. Song et al. (2023) investigated the resistance and motion of an AAMV in calm water and regular head waves using CFD and validated their predictions with towing tests of a scaled model, reporting average errors of 7.62%, 15.70% and 6.78% for resistance, pitch angle and heave, respectively. These figures illustrate both the usefulness and the limitations of numerical predictions of coupled AAMV behavior. The same study found that the AAMV had better seakeeping than the conventional high-speed planing craft considered. Song, Du, and Hu (2024) further showed that wind and waves can affect the motion stability of an AAMV, underlining the need to account for stability and operating limits in design. Resistance reduction has long been central to the optimization of HSMV performance, and computational techniques have played a critical role. Kim (1989) used potential-flow theory with Dawson's method to calculate ship flow and resistance and coupled it with optimization to minimize resistance, taking the wave-making resistance as the objective and the ship weight as the constraint. Zhang and Zhang (2015) later optimized the sum of the wave-making and viscous resistance using a non-linear programming method, with the displacement as the constraint. Their optimized hull form, obtained with the Rankine source method, was verified experimentally. Several other optimization approaches have also been investigated, including a surrogate-based method to reduce drag and improve seakeeping (Huang et al., 2015) and an improved particle swarm optimization (IPSO) algorithm combined with a neural network to minimize resistance (Zhang et al., 2018).

For high-speed vessels, Day and Doctors (1996) developed an optimization method that combined classical hill-climbing with a genetic algorithm (GA) to minimize total resistance subject to constraints on displacement, maximum local beam, required internal volume and maximum waterline slope. Jahanbakhsh et al. (2008) developed a numerical tool for simulating the hydrodynamics of high-speed planing craft. Mohamad Ayob et al. (2009) presented an optimization framework for the design

(This work is licensed under a Creative Commons Attribution 4.0 International License.)

International Journal of Engineering Research & Technology (IJERT)
ISSN: 2278-0181
Vol. 15 Issue 11 , November - 2026

of planing craft. Ayob et al. (2011) then optimized the hydrodynamic design of high-speed planing craft for coastal surveillance and later developed a preliminary hydrodynamic design optimization framework for such craft (Ayob et al., 2012). This framework is based on evolutionary algorithms, which are population-based search methods for single- and multi-objective optimization problems (Jin & Sendhoff, 2008; Jose & Vijayalakshmi, 2020). It uses the non-dominated sorting genetic algorithm II (NSGA-II) (Deb et al., 2002; Costa & Oliveira, 2003) as the underlying optimizer, together with a surrogate-assisted formulation, the evolutionary algorithm with spatially distributed surrogates (EASDS) (Isaacs et al., 2007). Ni et al. (2023) used the finite-volume CFD code STAR-CCM+ to simulate the forward motion of an ultra-high-speed AAMV with and without wings and validated the results against experimental data. They found that the aerodynamic components become a significant part of the total lift when the beam Froude number exceeds 6, which improves high-speed resistance and longitudinal motion stability. By comparing models with and without the aerodynamic wings, they explained the hybrid aero-hydrodynamic support mechanism of the vehicle. They also studied how the step configuration, spray rails and deadrise angle affect resistance, and found that double steps with spray rails give lower resistance at high speeds, while a planing surface with a variable deadrise angle further improves overall performance. Song et al. (2023) also developed a kinetic model of the AAMV in waves and a decoupled CFD-based model to study its resistance and motion at various speeds in calm water and regular head waves. They examined the flow around the aerodynamic wings and hydrodynamic steps to explain the aerodynamic alleviation mechanism, and compared the resistance, pitch and heave responses in calm water and in waves. More recently, Song, Du, and Hu (2024) studied numerically the motion stability of an AAMV under different sea states and wind conditions, while Song, Du, Jiang, and Hu (2024) investigated experimentally the longitudinal stability of a multi-step AAMV. These studies showed that the relative positions of the center of gravity and the center of pressure directly affect longitudinal stability, and they clarified how design parameters influence resistance and stability, providing a useful basis for AAMV optimization.

Research on AAMVs has thus progressed from mathematical modeling and conceptual development to increasingly detailed numerical and experimental investigations. Collu et al. (2007) formulated a unified mathematical model for high-speed hybrid air- and waterborne vehicles, laying the theoretical groundwork for analyzing configurations supported by both aerodynamic and hydrodynamic forces. Collu et al. (2009) subsequently developed a mathematical framework for designing HSMVs equipped with aerodynamic surfaces, and Collu et al. (2010) examined the relationship between the aerodynamic and hydrodynamic forces and longitudinal equilibrium. Recent studies have relied increasingly on CFD. Ni et al. (2023) demonstrated the growing importance of aerodynamic lift at high speeds and analyzed the influence of aerodynamic surfaces and hull features on resistance. Song et al. (2023) extended the analysis to regular head waves and combined CFD with scaled-model experiments, showing that both resistance and vessel motions must be considered. Song, Du, and Hu (2024) subsequently investigated AAMV stability in wind and waves, reinforcing the importance of stability in selecting aerodynamic configurations. In parallel, research on optimization has demonstrated its value in high-speed vessel design. Ayob et al. (2012) applied evolutionary optimization to high-speed planing craft, showing that it can search complex design spaces with competing hydrodynamic objectives. Other studies have sought to reduce the number of expensive objective-function evaluations through surrogate-assisted multi-objective algorithms (Aghaei Pour et al., 2024). Such developments are particularly relevant to AAMV design because high-fidelity CFD simulations are computationally demanding. However, these studies address either the aerodynamic treatment of purpose-built high-speed craft or the optimization of conventional high-speed vessels. The combination of existing-vessel conversion, aerodynamic alleviation, CFD and optimization remains largely unexplored. In summary, the literature shows that high-speed marine vessels can improve their performance through alternative hull configurations and lifting mechanisms, and that aerodynamic lift can supplement hydrodynamic support and influence resistance and vessel motions (Collu et al., 2009; Ni et al., 2023). Stability and wave conditions also play a key role in AAMV

(This work is licensed under a Creative Commons Attribution 4.0 International License.)

International Journal of Engineering Research & Technology (IJERT)
ISSN: 2278-0181
Vol. 15 Issue 11 , November - 2026

performance (Song, Du, & Hu, 2024; Song et al., 2023), and computational optimization can identify improved configurations for high-speed vessels (Ayob et al., 2011, 2012).

Nevertheless, a specific gap remains which is the systematic conversion and optimization of an existing high-speed passenger boat into an AAMV. Conventional vessel optimization has focused largely on hull form and hydrodynamic parameters, while most AAMV studies have dealt with conceptual or purpose-built ultra-high-speed vehicles. Few studies have combined aerodynamic modification with computational optimization using an existing passenger boat as the baseline configuration. The present study addresses this gap. It establishes the performance of an existing high-speed passenger boat, introduces an aerodynamic lifting surface, simulates the resulting configuration using CFD and optimizes the position of the surface before comparing the new configuration with the original vessel. The findings provide a basis for selecting the location and design of aerodynamic surfaces when converting existing high-speed boats.

2.0 NUMERICAL MODELING

Computational and analytical methods were used to investigate the feasibility of converting an existing high-speed passenger boat into an AAMV. The boat was characterized, its hull was modeled digitally from the collected geometric and operational data, and its performance was investigated numerically before and after an aerodynamic lifting surface was introduced. The baseline characteristics and performance of the selected boat were established first. A three-dimensional (3D) baseline model was created from the existing hull geometry and principal particulars, and this model served as the reference for the aerodynamic modification and the subsequent performance evaluation. The principal characteristics of the vessel were retained and the aerodynamic surface was introduced as the only modification, so that the conventional boat and its aerodynamically alleviated configuration could be compared directly. The effects of the modification were assessed in terms of hydrodynamic resistance, effective power, and aerodynamic lift and drag. SolidWorks was used for geometric modeling and ANSYS for the performance assessment and optimization. The theoretical models used to evaluate the principal performance characteristics of the baseline and converted boats are given in Eqs. (1)– (17). The CFD analysis followed standard practice.

- **Theoretical Models**

a. Resistance

The total resistance of the boat is the force required to overcome the fluid resistance during forward motion, and it is given by Eq. (1):

$$R_T = R_F + R_W + R_{APP} + R_A \quad (1)$$

Where:

R_T is the total resistance, R_F is the frictional resistance, R_W is the wave-making resistance, R_{APP} is the appendage resistance, and R_A is the air resistance.

Based on the ITTC-57/78 method, the total resistance of a ship can be estimated from Eq. (2):

$$R_T = C_{TS}\frac{1}{2}\rho {V_S}^2 S_s \quad (2)$$

and

(This work is licensed under a Creative Commons Attribution 4.0 International License.)

International Journal of Engineering Research & Technology (IJERT)
ISSN: 2278-0181
Vol. 15 Issue 11 , November - 2026

$$C_{TS} = C_{FS} + C_R \text{ (here, } C_R = C_{RS} = C_{RM}) \quad (3)$$

The total resistance coefficient, C_T, is extrapolated from the model test result on the assumption that the residuary resistance of the model, C_{RM}, is equivalent to that of a ship, C_{RS}, as expressed in Eq. (3).

At low Froude numbers (Fr ≤ 0.12), frictional resistance accounts for about 85% of the total resistance, whereas at high Froude numbers it accounts for 40–50%. The frictional resistance depends on the Reynolds number of the flow around the hull, the wetted surface area and the density of the water. The frictional resistance coefficient and the Reynolds number are given by Eqs. (4) and (5):

$$C_F = \frac{0.075}{(LogR_n - 2)^2} \quad (4)$$

$$R_n = \frac{V_S . L_{WL}}{\vartheta} \quad (5)$$

The total resistance coefficient, C_T, is given by Eq. (6):

$$C_T = \frac{R_T}{\frac{1}{2}\rho {V_S}^2 S_S} \quad (6)$$

Where:

ρ is the density of water, V_S is the vehicle speed, and S_S is the wetted surface area.

For the high-speed operating condition, the Froude number is calculated from Eq. (7):

$$Fr = \frac{V_S}{\sqrt{gL}} \quad (7)$$

where:

Fr is the Froude number, g is the gravitational acceleration and L is the characteristic length of the vessel. The resistance of the baseline and modified configurations was compared at the same speed to assess the effect of aerodynamic alleviation.

b. Lift Model

For HSMVs, the hydrodynamic lift depends on speed and is given by Eq. (8):

$$L_{Hydro} = K_{LH} \times \rho_{water} \times {V_B}^2 \times S_{sH} \quad (8)$$

For an AAMV, the total lift, L_{total}, is the sum of the hydrodynamic and aerodynamic lift components, as shown in Eq. (9):

$$L_{total} = K_{HA} \times \left(L_{Hydro} + L_{AERO}\right) \quad (9)$$

The aerodynamic lift is formulated in the same way as the hydrodynamic lift and is given by Eq. (10):

(This work is licensed under a Creative Commons Attribution 4.0 International License.)

International Journal of Engineering Research & Technology (IJERT)
ISSN: 2278-0181
Vol. 15 Issue 11 , November - 2026

$$L_{AERO} = K_{LA} \times \rho_{Air} \times {V_B}^2 \times S_{sA} \quad (10)$$

Where:

L_{Hydro} is the hydrodynamic lift, L_{AERO} is the aerodynamic lift, K_{LH} is the hydrodynamic lift coefficient, K_{LA} is the aerodynamic lift coefficient, ρ_{water} is the density of water, ρ_{Air} is the density of air, V_B is the speed of the boat, S_{sH} and S_{sA} are the surface areas of the submerged hull and the aerodynamic surfaces, respectively. In Eq. (9), K_{HA} is a correction factor that accounts for the interaction between the hydrodynamic and aerodynamic lift components. K_{HA} = 1 when the two components do not interact. In the present study the interaction was not prescribed through K_{HA}; it was resolved directly by the coupled air–water CFD solution.

c. Effective Power Model

The power required to overcome the total resistance at a given speed is the effective power, given by Eq. (11):

$$P_E = R_T V_S \quad (11)$$

d. Efficiency Model

The aerodynamic efficiency of the wing is assessed using the lift-to-drag ratio in Eq. (12):

$$\frac{L_A}{D_A} = \frac{C_L}{C_D} \quad (12)$$

Where:

L_A and D_A represent the aerodynamic lift and drag of the wing, respectively (L_A is the same quantity as L_{AERO} in Eq. (10)), while C_L and C_D are the corresponding lift and drag coefficients; this parameter indicates how effectively the aerodynamic surfaces generate useful lift relative to the aerodynamic drag introduced by the modification. The overall improvement was evaluated by comparing the resistance and power requirement of the baseline and optimized configurations.

e. Stability Model

Stability must be considered because an aerodynamic surface changes the distribution of forces and moments acting on the vessel. In particular, aerodynamic lift acts above the waterline and generates pitching moments that influence trim and longitudinal stability.

The aerodynamic pitching moment is expressed as:

$$M_A = L_A x_L - D_A z_D \quad (13)$$

Where:

(This work is licensed under a Creative Commons Attribution 4.0 International License.)

International Journal of Engineering Research & Technology (IJERT)
ISSN: 2278-0181
Vol. 15 Issue 11 , November - 2026

M_A is the aerodynamic pitching moment, L_A is the aerodynamic lift, D_A is the aerodynamic drag, x_L is the longitudinal moment arm of the lift force and z_D is the vertical moment arm of the drag force relative to the selected reference point.

The longitudinal equilibrium is described by the balance between the weight of the vessel, the hydrostatic buoyancy and the hydrodynamic and aerodynamic lift:

$$W = B + L_{Hydro} + L_{AERO} \quad (14)$$

Where:

W is the weight of the boat, B is the hydrostatic buoyancy, L_{Hydro} is the hydrodynamic lift, and L_{AERO} is the aerodynamic lift, as defined in Eqs. (8) and (10).

The trim, pitch and, where applicable, heave response are therefore relevant to the stability of the converted vessel. This is particularly important because previous AAMV studies have shown that the relative positions of the center of gravity and the aerodynamic center influence longitudinal stability (Collu et al., 2010; Song, Du, Jiang, & Hu, 2024). Equations (13) and (14) provide the basis for this assessment. In the present study, the configurations were compared on the basis of resistance and lift, and a full stability assessment is left for future work.

The percentage improvement in the principal performance parameters was calculated using:

$$\%\ Improvement = \frac{X_{baseline} - X_{AAMV}}{X_{baseline}} \times 100 \quad (15)$$

- **Performance Evaluation**

The optimized configuration was evaluated under the same operating conditions and with the same numerical procedure as the original passenger boat. The comparison covered the total resistance, the effective power and the aerodynamic lift and drag of the wing.

The percentage change in resistance was calculated as:

$$\%\Delta R = \frac{R_{baseline} - R_{optimized}}{R_{baseline}} \times 100 \quad (16)$$

Similarly, the percentage change in propulsion power was calculated as:

$$\%\Delta P = \frac{P_{baseline} - P_{optimized}}{P_{baseline}} \times 100 \quad (17)$$

- **Governing Equations and Turbulence Modeling**

The flow is governed by the time-averaged continuity and momentum equations for incompressible flow with external forces, Eqs. (18) and (19):

$$\frac{\partial(\rho \bar{u}_i)}{\partial x_i} = 0 \quad (18)$$

(This work is licensed under a Creative Commons Attribution 4.0 International License.)

International Journal of Engineering Research & Technology (IJERT)
ISSN: 2278-0181
Vol. 15 Issue 11 , November - 2026

$$\frac{\partial(\rho\bar{\bar{u}}_i)}{\partial t} + \frac{\partial}{\partial xj}\left(\rho\bar{u}_i\bar{\bar{u}}_j + \rho\overline{u_i{}'u_j{}'}\right) = -\frac{\partial\bar{\bar{p}}}{\partial x_i} + \frac{\partial\bar{\tau}_{ij}}{\partial x_i} \quad (19)$$

Where:

$\bar{\bar{u}}_i$ is the mean velocity of the flow relative to the control volume,

$\overline{u_i{}'u_j{}'}$ is the Reynolds stress tensor,

$\bar{\bar{p}}$ is the mean pressure, and

$\bar{\tau}_{ij}$ is the mean viscous stress tensor for a Newtonian fluid under the incompressible flow assumption.

The stress tensor $\bar{\tau}_{ij}$ is given by Eq. (20):

$$\bar{\tau}_{ij} = \mu\left(\frac{\partial\bar{u}_i}{\partial x_j} + \frac{\partial\bar{u}_j}{\partial x_i}\right) \quad (20)$$

Because the problem involves two-phase flow, the volume of fluid (VOF) multiphase model was adopted, with second-order spatial and temporal discretization schemes and an implicit VOF formulation. The general transport equation for the multiphase flow is given by Eq. (21):

$$\frac{\partial(\alpha\rho\varphi)}{\partial t} + \nabla.\left(\alpha\rho\vec{V}\varphi\right) = \nabla.\bar{\bar{\tau}} + S_\varphi \quad (21)$$

Where:

φ is the phase variable, α is the phase volume fraction, ρ is the mixture density (which differs for air and water), $\vec{V}$ is the phase velocity, $\bar{\bar{\tau}}$ is the diffusion term, and S_φ is the source term.

A fully implicit scheme was used, in which Eq. (21) was discretized in time with the second-order backward Euler approximation, giving:

$$\frac{3\left(a_p\rho_p\varphi_p Vol\right)^{n+1} - 4\left(a_p\rho_p\varphi_p Vol\right)^{n} + \left(a_p\rho_p\varphi_p\right)^{n-1}}{2\Delta t} =$$

$$\sum[A_{nb}(\varphi_{nb} - \varphi_p)]^{n+1} + {S_U}^{n+1} - {S_p}^{n+1}{\varphi_p}^{n+1} \quad (22)$$

(This work is licensed under a Creative Commons Attribution 4.0 International License.)

International Journal of Engineering Research & Technology (IJERT)
ISSN: 2278-0181
Vol. 15 Issue 11 , November - 2026

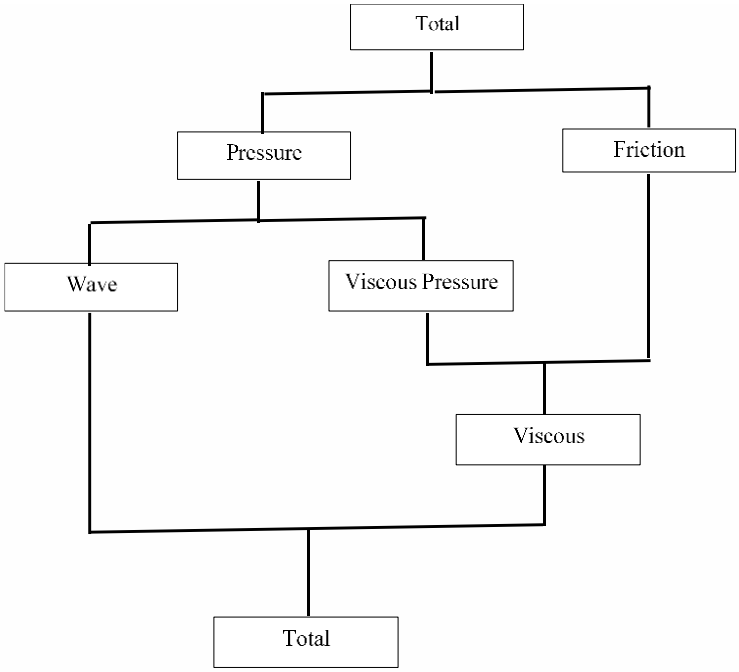

Figure 2: Flow chart of the CFD simulation of resistance (adapted from Molland et al., 2011)

- **Validation Study**

To validate the numerical model, a hull form previously simulated by Ohwofadjeke et al. (2024) was used as the first case (Case A), its particulars and boundary settings are given in Table 1. The second case (Case B), for which only the total resistance was investigated, was based on the planing hull studied by Pacuraru et al. (2022), its particulars are given in Table 2.

Table 1: Principal particulars of validation Case A (Ohwofadjeke et al., 2024)

Description	Value
Hull form type	Square flat edge
Length (m)	1.9
Breadth (m)	0.4
Draft (m)	0.3
Speed (kn) [m/s]	6 [3.086]

Table 2: Principal particulars of validation Case B (Pacuraru et al., 2022)

Description	Value
Length overall (m)	2.611
Draft (m)	0.168
Beam at waterline (m)	0.743
Longitudinal center of gravity, LCG (m)	0.944
Displacement (kg)	106.7
Mean deadrise angle (deg)	14
Speeds (m/s)	2.0 – 7.5

(This work is licensed under a Creative Commons Attribution 4.0 International License.)

International Journal of Engineering Research & Technology (IJERT)
ISSN: 2278-0181
Vol. 15 Issue 11 , November - 2026

- **Optimization Procedure**

The input design variables for the conversion of an HSMV include the geometry, location, surface area and orientation of the aerodynamic alleviation surface (wing), while the output variables are the hydrodynamic resistance and lift of the hull and the aerodynamic lift and drag of the wing. The optimization procedure of Fiala et al. (2022) was adopted. It has two phases: a design phase, divided into three parts, and an implementation phase, divided into five parts, as shown in Figure 3. Constraints are needed to exclude solutions that give favorable numerical resistance but are impractical operationally from a stability standpoint. Because the objectives may conflict, a multi-objective formulation is appropriate. For instance, increasing the area of the aerodynamic surface increases lift but also increases aerodynamic drag and changes the pitching moment. Similarly, the configuration with the lowest resistance may not have the most favorable stability characteristics. Multi-objective methods are useful because they identify a set of non-dominated solutions without reducing all objectives to a single function. The optimization was carried out after the CFD models of the baseline and modified vessels had been developed. Its aim was to identify the parameters of the aerodynamic surface that improve vessel performance relative to the original configuration, after which the optimal design was evaluated in detail. Although the geometry, area and incidence of the wing are all potential design variables, in this study the design variables were the longitudinal, transverse and vertical (X, Y, Z) coordinates of the wing, with its geometry and angle of attack held fixed (Table 3). The design space was bounded by practical geometric and operational limits.

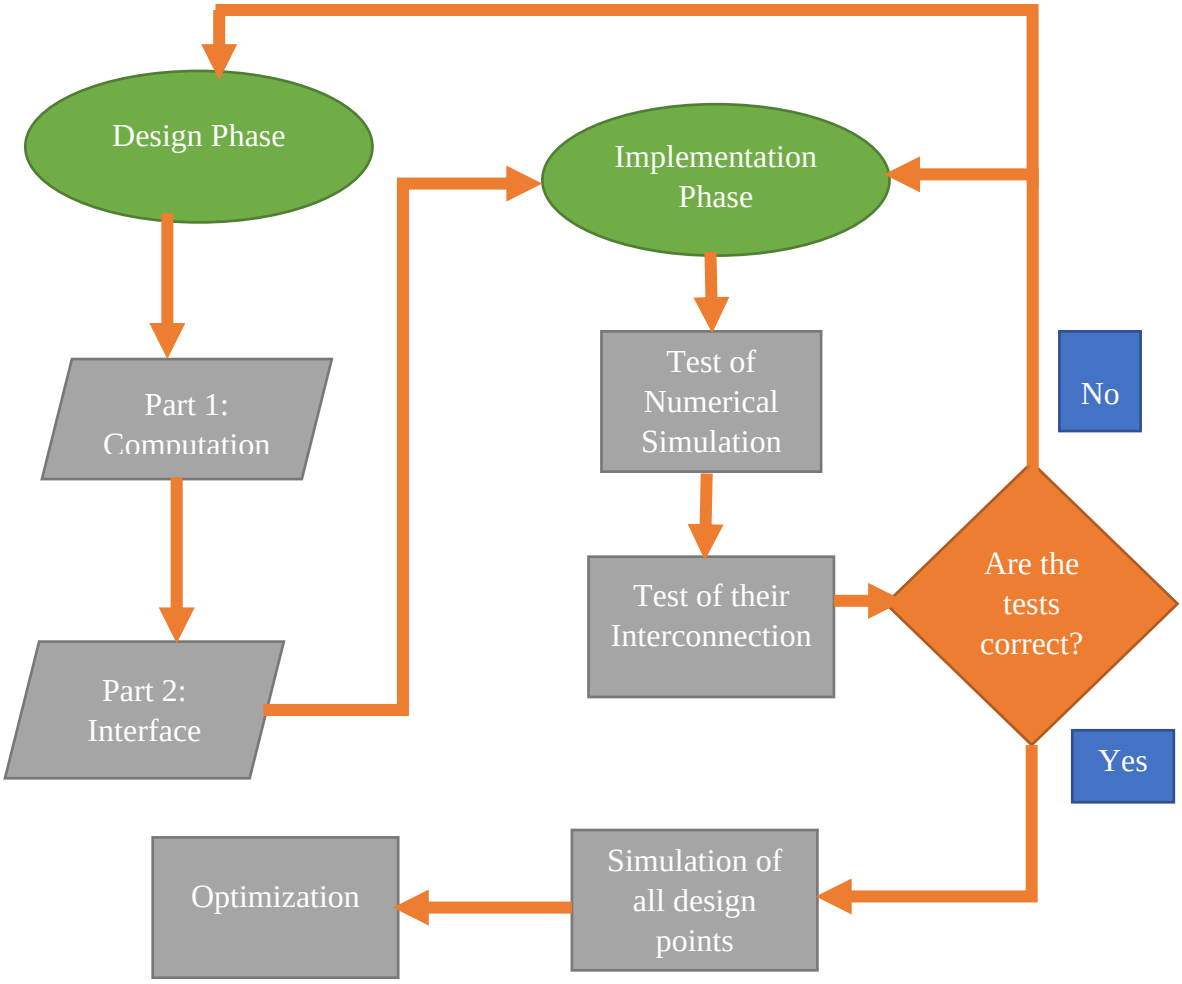

Figure 3: Flowchart of the optimization procedure

(This work is licensed under a Creative Commons Attribution 4.0 International License.)

International Journal of Engineering Research & Technology (IJERT)
ISSN: 2278-0181
Vol. 15 Issue 11 , November - 2026

The principal objective was to reduce the total resistance or the propulsion power while maintaining sufficient lift. The objective function was therefore formulated as Eq. (23):

$$min\ f(x) = R_T(x) \tag{23}$$

or, where a combined objective was required,

$$min\ f(x) = w_1 R_T(x) + w_2 P_E(x) \tag{24}$$

Where:

x is the vector of design variables, and w_1 and w_2 are weighting coefficients, and P_E is the effective power defined in Eq. (11).

The optimization was performed with the screening multi-objective direct optimization method in ANSYS. Ten design points were generated as a preliminary investigation and ranked against the performance criteria using the defined objective function and constraints. The best candidate point was then re-simulated with a final high-fidelity CFD analysis to obtain the results. The selected passenger boat was first reproduced as a 3D CAD model in SolidWorks. The model included the hull surfaces above and below the waterline required for the hydrodynamic analysis. The aerodynamic surface was then added to the baseline geometry in SolidWorks, so that the conversion started from the existing hull model. The baseline geometry was first simulated in ANSYS to establish the performance of the original configuration, focusing on resistance and powering. Figure 4 shows the initial assembly of the planing hull with the wing attached at the reference location, which was taken as the origin (0, 0, 0) of the x, y and z coordinates. The lower and upper bounds of the wing position were set to −1.5 m and 0 m for x, 0 m and 0.2 m for y, and −0.5 m and 0 m for z, measured from the reference location.

The principal particulars of the model-scale hull and the wing are given in Table 3.

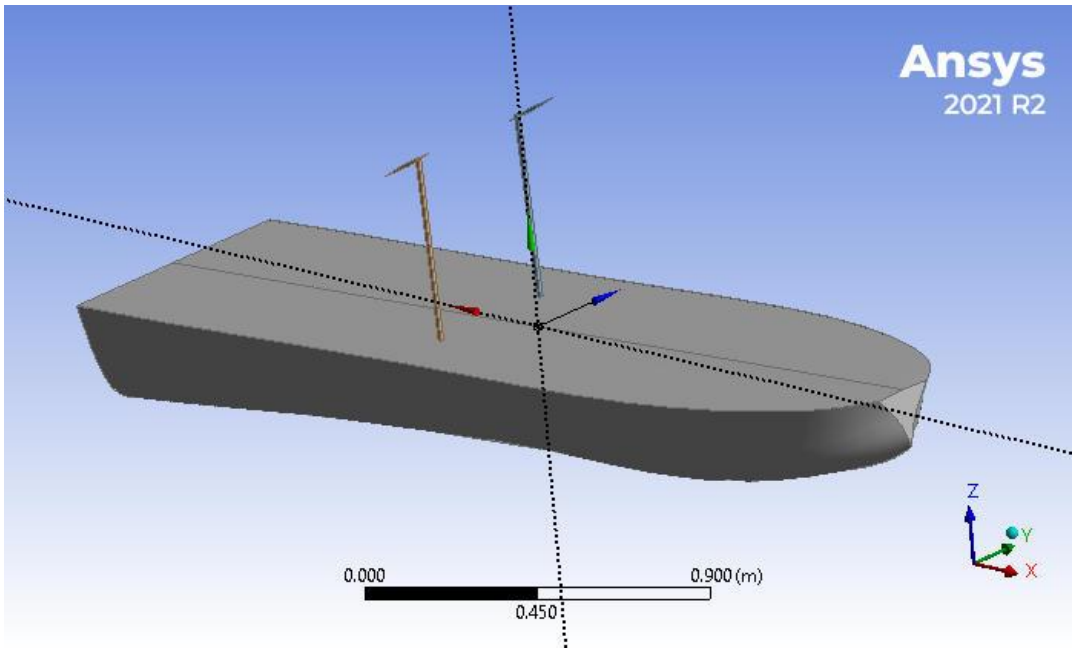

Figure 4: Initial hull design with the wing attached at the reference location

(This work is licensed under a Creative Commons Attribution 4.0 International License.)

International Journal of Engineering Research & Technology (IJERT)
ISSN: 2278-0181
Vol. 15 Issue 11 , November - 2026

Table 3: Principal features of the hull and wing

Parameter	Value
Hull	
Scale	2.3
Length overall (m)	2.61
Beam (m)	0.7
Depth (m)	0.32
Draft (m)	0.2
Speed (m/s)	7.1
Wing	
Length (m)	0.09
Angle of attack (deg)	15
Maximum thickness (m)	0.0025

3.0 RESULTS AND DISCUSSION

For Case A, the total resistance was obtained from the total resistance coefficient computed with the realizable k–ε turbulence model and standard wall functions. The simulation assumed calm water with no wave generation.

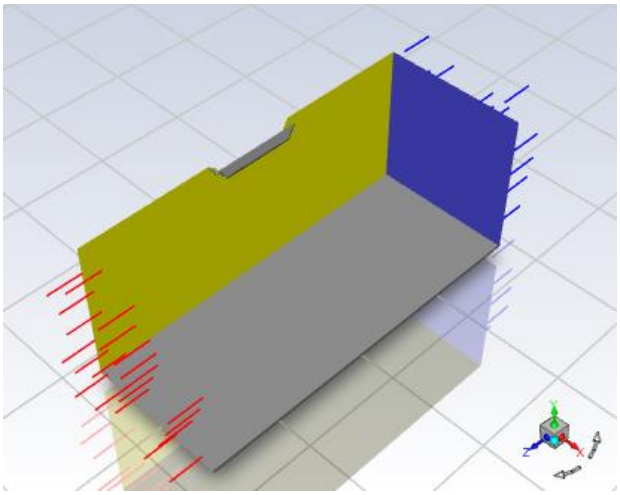

Figure 5: Computational model of validation Case A

The total resistance was 945.97 N, 979.17 N and 977.84 N for the unstructured mesh, the structured mesh and the structured mesh with an outflow boundary condition, respectively. The type and resolution of the mesh therefore have a clear influence on the predicted resistance. Figures 6(a) and 6(b) compare the surface area reported by Ohwofadjeke et al. (2024) with that of the model reproduced in this study using the same principal dimensions. The two differ by about 50%, which shows that the reproduced geometry is not identical to the reference hull. This geometric difference carries through to the total resistance coefficient, which differs by about 82% (Figures 6(c) and 6(d)), and to the total resistance (Figures 6(e) and 6(f)). Case A was therefore used mainly to assess the sensitivity of the solution to mesh type and boundary conditions, while Case B, for which the hull particulars are fully specified, was used to check the accuracy of the resistance prediction.

(This work is licensed under a Creative Commons Attribution 4.0 International License.)

International Journal of Engineering Research & Technology (IJERT)
ISSN: 2278-0181
Vol. 15 Issue 11 , November - 2026

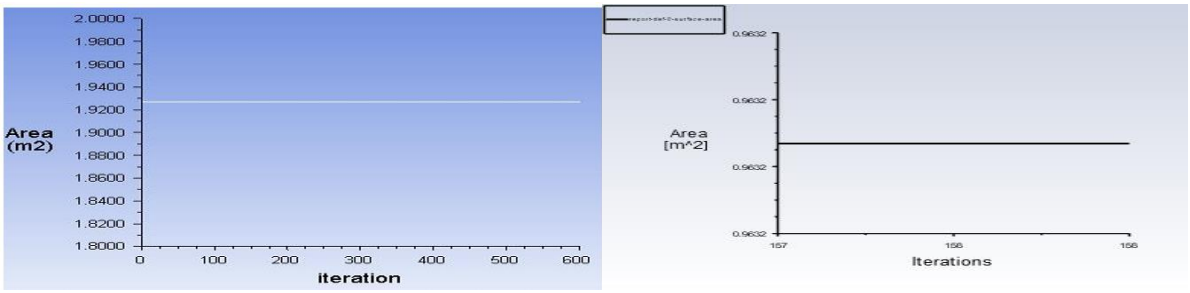

Figure 6: (a) Surface area of Case A reported by Ohwofadjeke et al. (2024) and (b) surface area of Case A in the present study

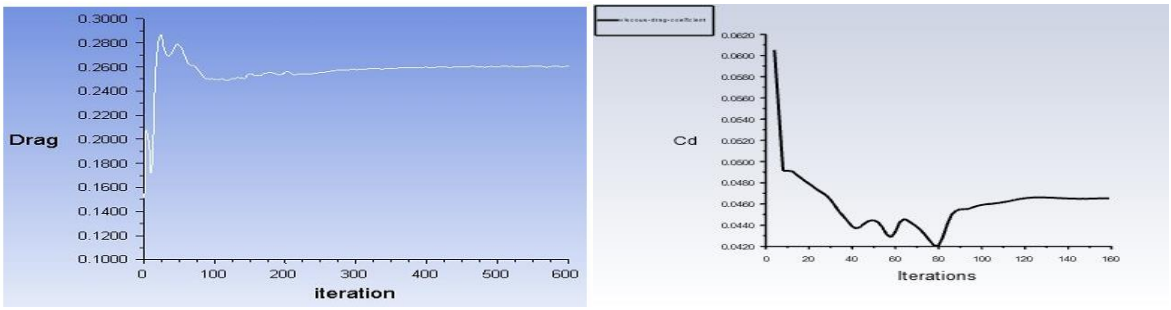

Figure 6: (c) Total resistance coefficient of Case A reported by Ohwofadjeke et al. (2024) and (d) total resistance coefficient of Case A in the present study

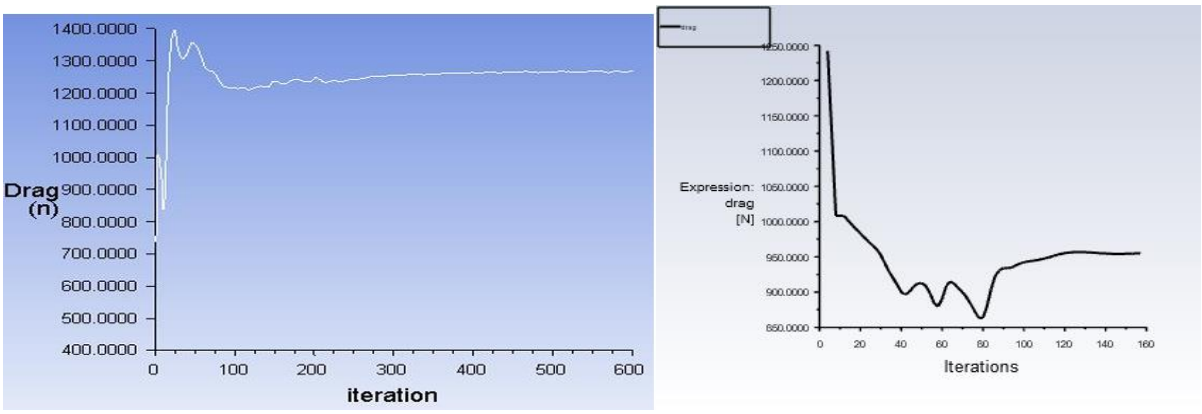

Figure 6: (e) Total resistance of Case A reported by Ohwofadjeke et al. (2024) and (f) total resistance of Case A in the present study

Figure 7(a)–(d) shows the influence of the mesh on the resistance coefficient and the total resistance for this case. The first structured mesh appears to over-predict both quantities, whereas the structured mesh with an outflow boundary condition gives more conservative values. Mesh type, mesh size and boundary conditions are therefore critical to the accuracy of the numerical model.

(This work is licensed under a Creative Commons Attribution 4.0 International License.)

International Journal of Engineering Research & Technology (IJERT)
ISSN: 2278-0181
Vol. 15 Issue 11 , November - 2026

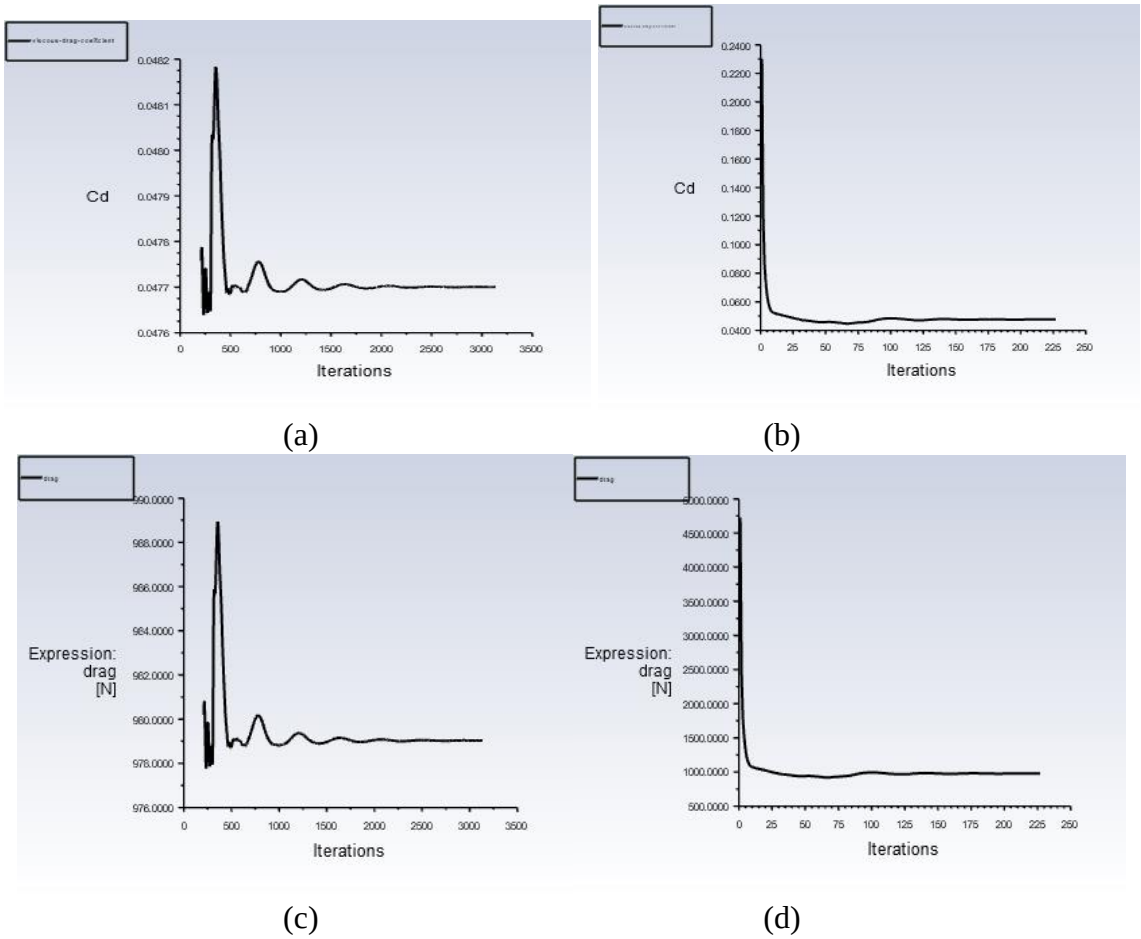

Figure 7: (a), (b) Total resistance coefficients and (c), (d) total resistance for the two structured meshes

The computational model for Case B is shown in Figure 8. The resistance was computed at a speed of 2.5 m/s, and convergence was judged from both the residuals and the moment coefficient, C_m, which reached a steady value as shown in Figure 9. The converged total resistance was 80 N, which is close to the value reported by Pacuraru et al. (2022) (Figure 10). This agreement indicates that the numerical setup can predict the resistance of a planing hull with acceptable accuracy. A formal mesh-independence study was not carried out for the converted boat, and this is identified as a limitation of the present results.

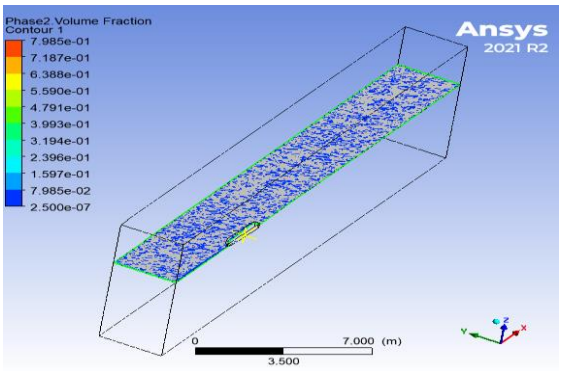

Figure 8: Computational model of validation Case B

(This work is licensed under a Creative Commons Attribution 4.0 International License.)

International Journal of Engineering Research & Technology (IJERT)
ISSN: 2278-0181
Vol. 15 Issue 11 , November - 2026

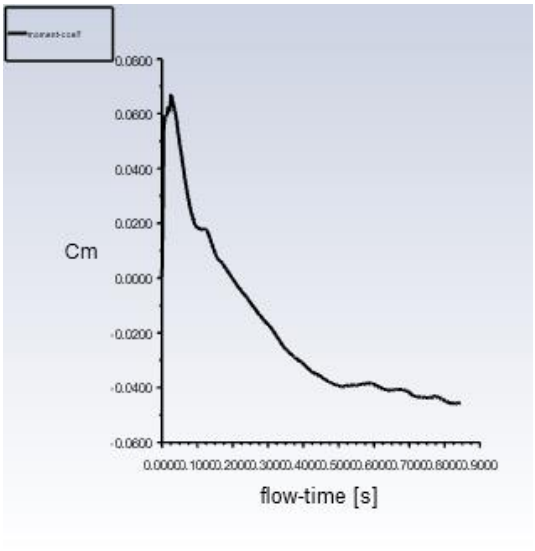

Figure 9: Convergence history of the moment coefficient, C_m

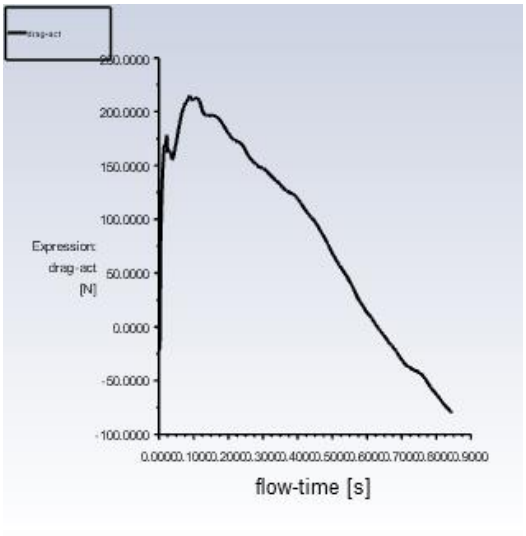

Figure 10: Total resistance of Case B

The HSMV was modeled together with a wing-like body representing the aerodynamic surface. In preliminary simulations, the height of the wing above the hull and its angle of attack were varied. These showed that the hydrodynamic resistance decreases as the angle of attack increases, while both the hydrodynamic and the aerodynamic lift increase. A screening optimization was then used to investigate the influence of the wing position on the hydrodynamic and aerodynamic resistance and lift. The lower and upper limits of the three coordinates were set, together with the objectives and target values of these quantities, and the optimization was run with 10 design points. Figure 11 shows the optimization dashboard. Three candidate points were obtained, of which candidate point 2 is the global optimum, with the lowest hydrodynamic resistance and the highest hydrodynamic lift. Figure 12 shows further results that are not visible in the dashboard: candidate point 2 is 2.04% better than candidate point 3, and candidate point 1 is 0.61% better than candidate point 3. Candidate point 2 also has 70.30% lower aerodynamic resistance than candidate point 3, although its aerodynamic lift is also lower.

(This work is licensed under a Creative Commons Attribution 4.0 International License.)

International Journal of Engineering Research & Technology (IJERT)
ISSN: 2278-0181
Vol. 15 Issue 11 , November - 2026

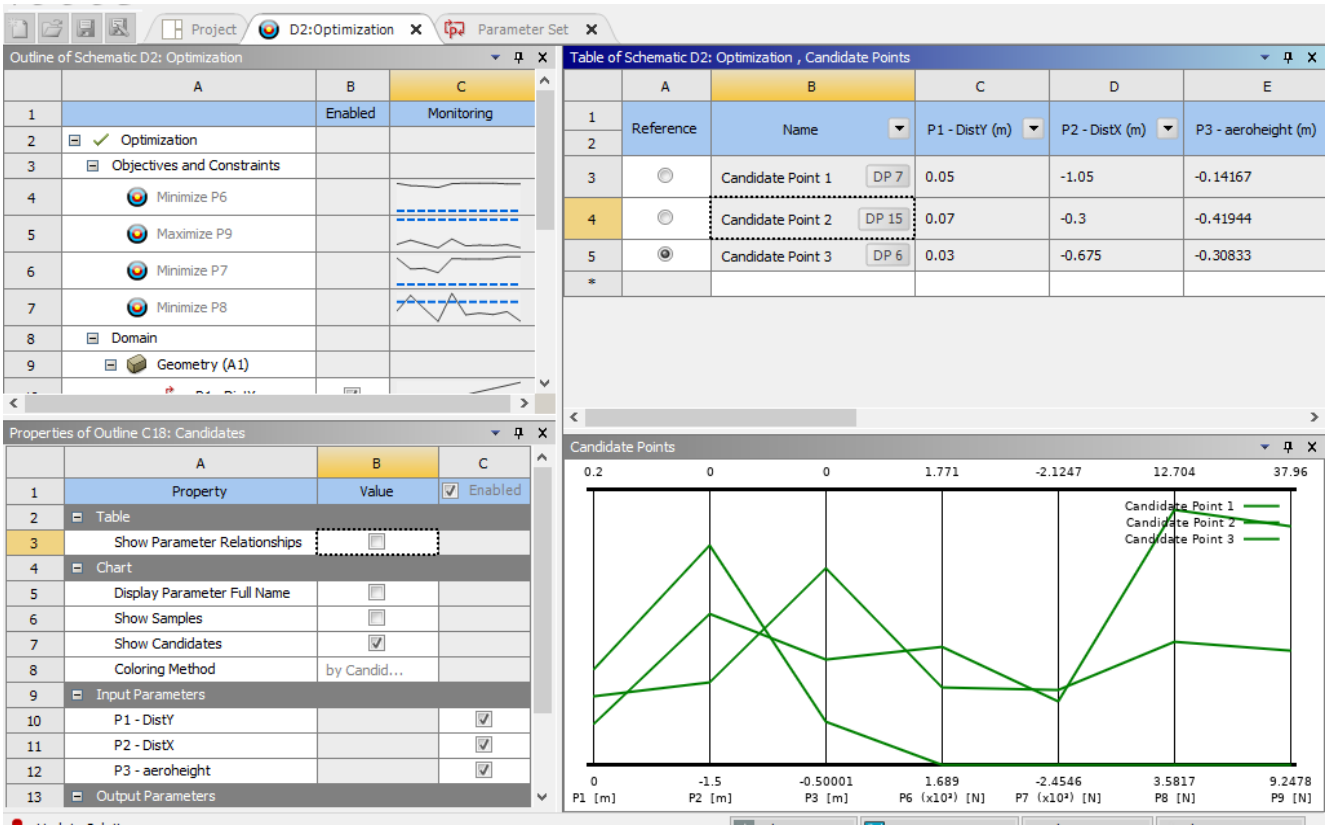

Figure 11: Optimization dashboard

P6 - HullResistanceF (N)		P7 - HullHydroLift (N)		P8 - WingAeroResistance (N)	
Parameter Value	Variation from Reference	Parameter Value	Variation from Reference	Parameter Value	Variation from Re
1712.3	-0.69%	-2363.7	0.61%	7.677	-36.35%
1689	-2.04%	-2454.6	-3.21%	3.5818	-70.30%
1724.2	0.00%	-2378.3	0.00%	12.061	0.00%

Figure 12 (a): Optimization results for the candidate points

L	M	C	D	E
P9 - WingAeroLift (N)		P1 - DistY (m)	P2 - DistX (m)	P3 - aeroheight (m)
Parameter Value	Variation from Reference			
21.162	-38.02%	0.05	-1.05	-0.14167
9.2478	-72.92%	0.07	-0.3	-0.41944
34.145	0.00%	0.03	-0.675	-0.30833
		0.1	*-0.75*	*-0.25*

Figure 12 (b): Optimization results for the candidate points (continued)

(This work is licensed under a Creative Commons Attribution 4.0 International License.)

International Journal of Engineering Research & Technology (IJERT)
ISSN: 2278-0181
Vol. 15 Issue 11 , November - 2026

Figure 13 shows the feasible design points of the optimization. On the basis of these results, the optimal design was obtained at candidate point 2, with the wing located at X = -0.3 m, Y = 0.07 m and Z = -0.41944 m.

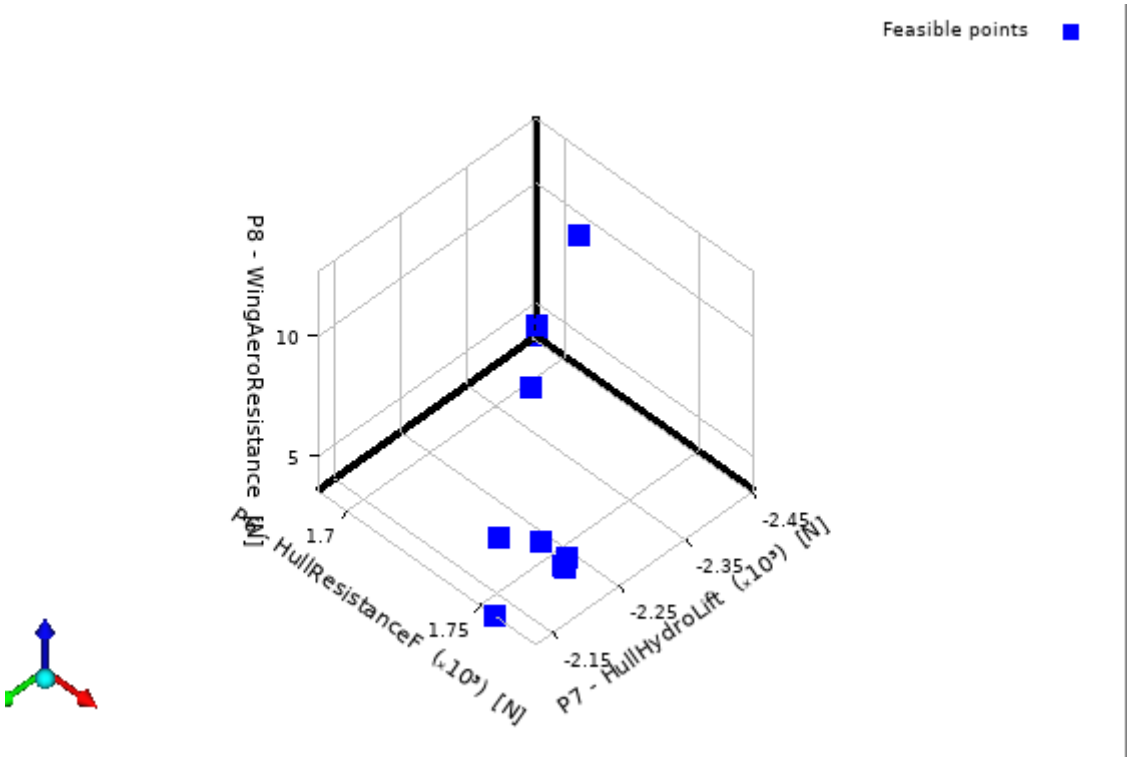

Figure 13: Feasible design points of the optimization

A further simulation was performed at this point to obtain the flow field and the hydro-aerodynamic performance of the converted boat. Figures 14 and 15 show the velocity, pressure and turbulence kinetic energy, and Figures 16–19 show the hydro-aerodynamic performance. At the optimum, the hydrodynamic resistance was 1689 N, the hydrodynamic lift 2454.6 N, the wing drag 9.25 N and the wing lift 3.58 N. Compared with the boat without the wing (1809 N), the hydrodynamic resistance was reduced by 6.6%. When the wing drag is included, the total resistance is 1698.2 N, a reduction of 6.1%. At the design speed of 7.1 m/s, this corresponds to a reduction in effective power (Eq. 11) from 12.84 kW to 12.06 kW at model scale. Because the lift and drag of the wing itself are small compared with the hydrodynamic forces, the reduction in hull resistance appears to arise mainly from the interaction of the wing with the flow around the hull rather than from a direct transfer of lift. At the design speed, the wing lift is only about 0.15% of the hydrodynamic lift, so the converted boat lies at the lower edge of the aerodynamic alleviation zone. A larger wing area or a higher operating speed would be needed for the aerodynamic lift to carry a significant share of the weight (Ni et al., 2023).

(This work is licensed under a Creative Commons Attribution 4.0 International License.)

International Journal of Engineering Research & Technology (IJERT)
ISSN: 2278-0181
Vol. 15 Issue 11 , November - 2026

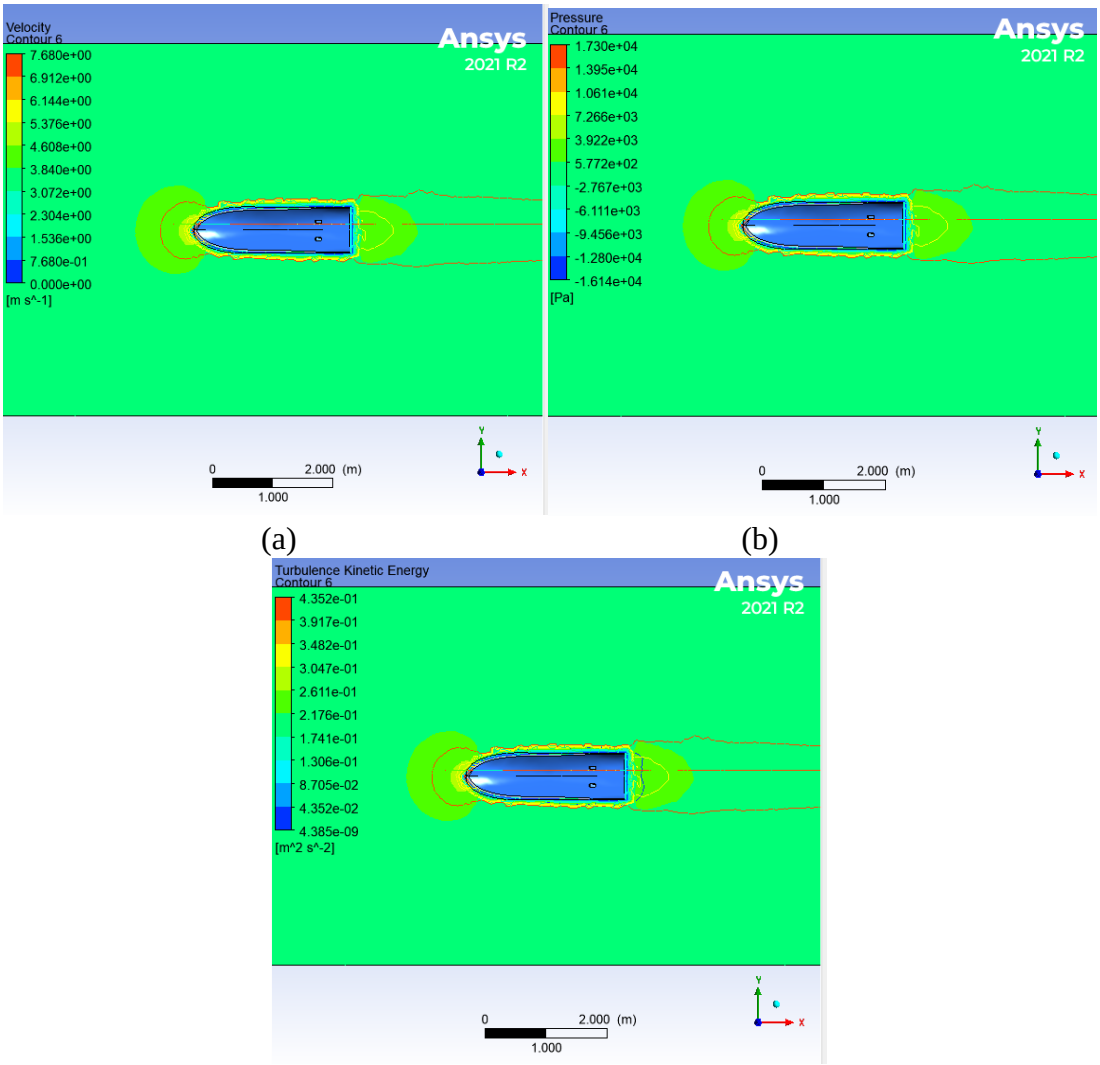

(a) (b)

(c)

Figure 14: (a) Velocity, (b) pressure and (c) turbulence kinetic energy on the water surface at the optimal configuration

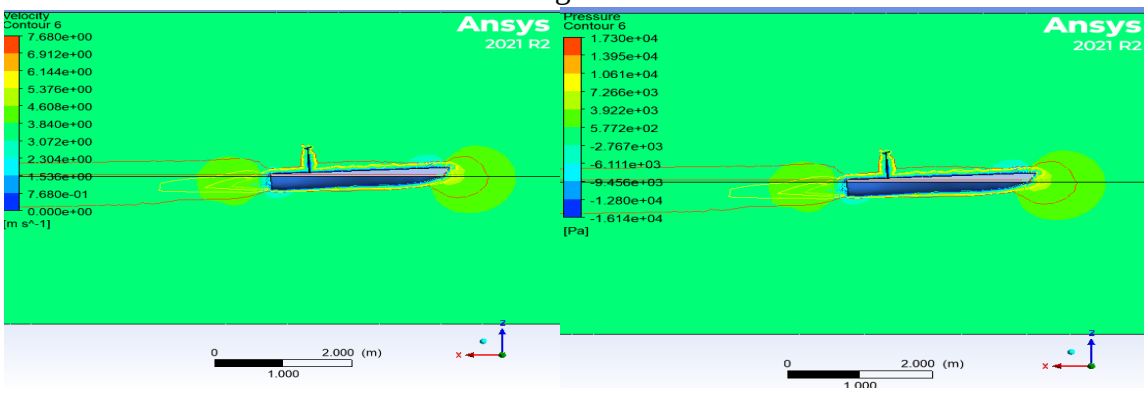

(a) (b)

(This work is licensed under a Creative Commons Attribution 4.0 International License.)

International Journal of Engineering Research & Technology (IJERT)
ISSN: 2278-0181
Vol. 15 Issue 11 , November - 2026

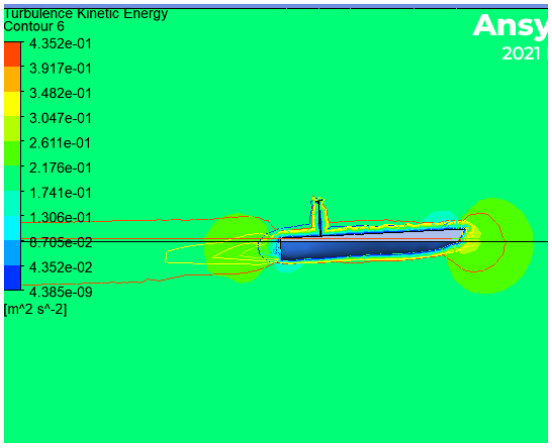

(c)

Figure 15: (a) Velocity, (b) pressure and (c) turbulence kinetic energy profiles at the optimal configuration (side view)

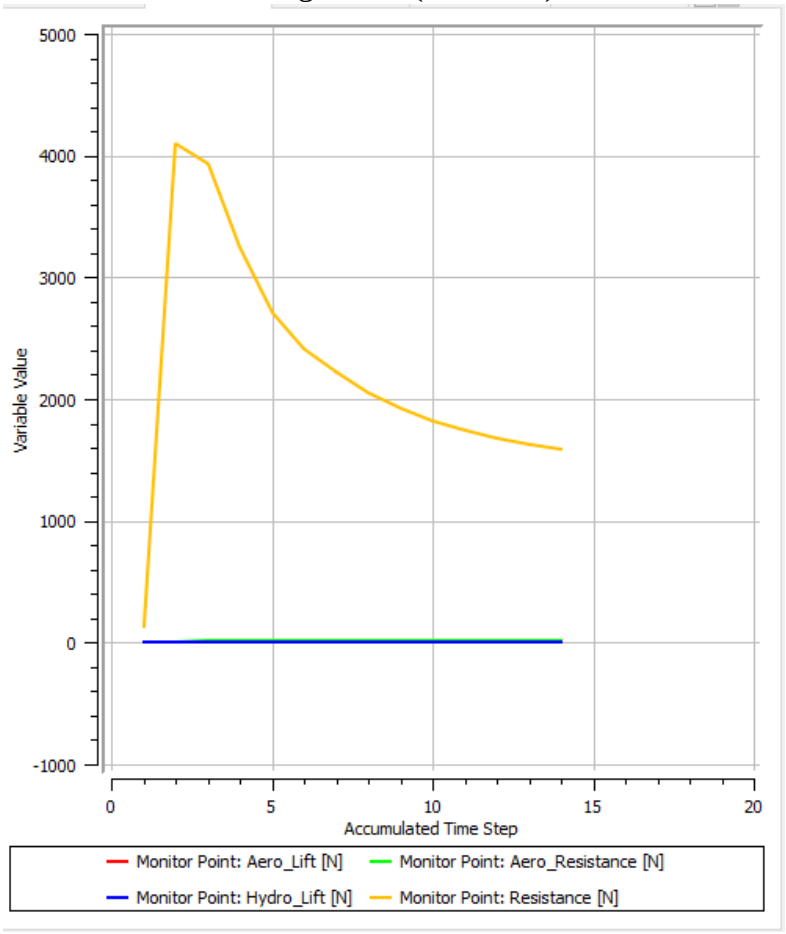

Figure 16: Hydro-aerodynamic performance characteristics

(This work is licensed under a Creative Commons Attribution 4.0 International License.)

International Journal of Engineering Research & Technology (IJERT)
ISSN: 2278-0181
Vol. 15 Issue 11 , November - 2026

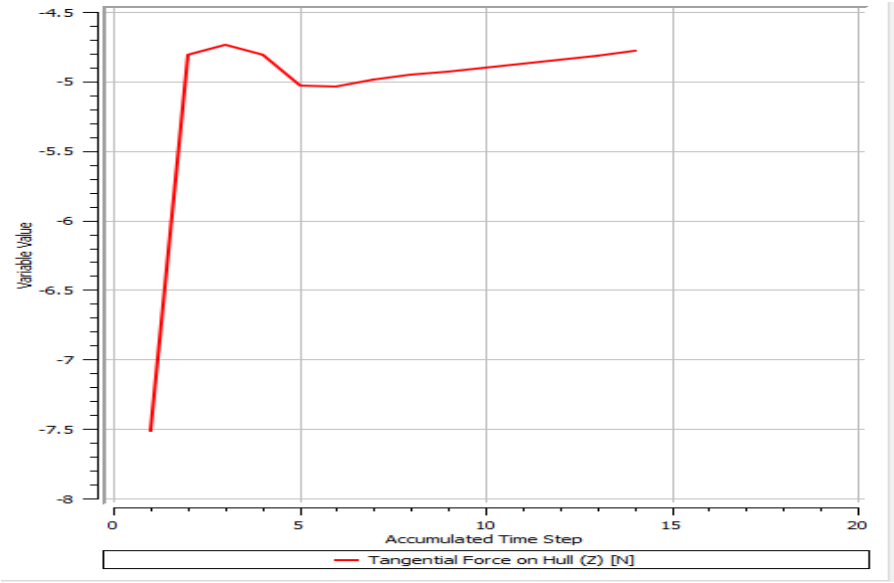

Figure 17: Hydrodynamic lift

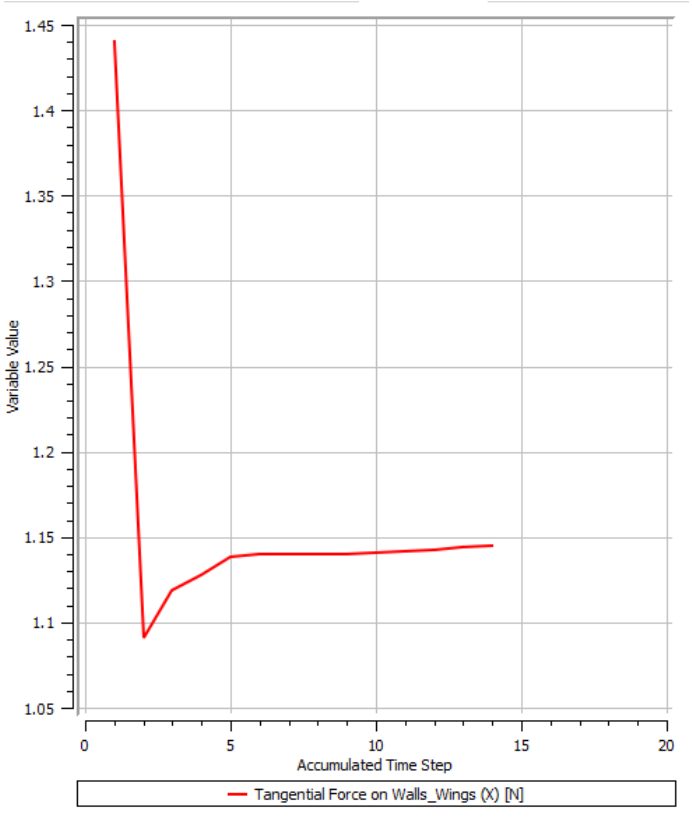

Figure 18: Aerodynamic resistance

(This work is licensed under a Creative Commons Attribution 4.0 International License.)

International Journal of Engineering Research & Technology (IJERT)
ISSN: 2278-0181
Vol. 15 Issue 11 , November - 2026

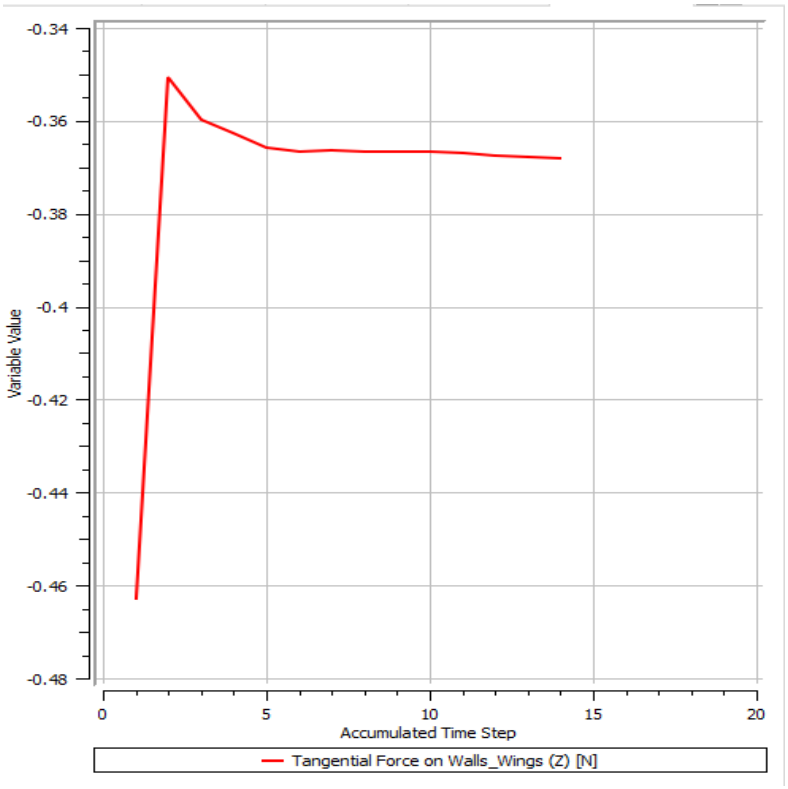

Figure 19: Aerodynamic lift

CONCLUSION

Converting an HSMV into an AAMV with a gain in performance requires reliable numerical predictions. This study therefore paid particular attention to numerical accuracy through validation against two published cases. The following conclusions can be drawn:

(i) Numerical error is inherent in resistance simulations and it can be reduced by careful choice of boundary conditions, mesh size and mesh type.

(ii) In converting HSMVs to AAMVs, it is essential to determine the best location and angle of attack of the aerodynamic surface.

(iii) The hydrodynamic resistance decreases as the angle of attack of the wing increases, while the lift varies with the location of the wing.

(iv) At the optimal wing location (candidate point 2: X = -0.3 m, Y = 0.07 m, Z = -0.41944 m), the hydrodynamic resistance of the model fell from 1809 N without the wing to 1689 N, a reduction of about 6.6%, and the total resistance including the wing drag fell by about 6.1%. An existing high-speed passenger boat can therefore be converted into an AAMV with a measurable gain in hydrodynamic performance.

RECOMMENDATIONS

The following recommendations are made for future work based on the limitations of the study:

i. Verification and validation should be extended to benchmark cases such as those published by the ITTC.

ii. A mesh-independence study, for example using the grid convergence index, should be carried out for the baseline and converted boats.

(This work is licensed under a Creative Commons Attribution 4.0 International License.)

International Journal of Engineering Research & Technology (IJERT)
ISSN: 2278-0181
Vol. 15 Issue 11 , November - 2026

iii. The influence of other wing and hull parameters, including wing area, span and angle of attack, on performance should be investigated using advanced optimization methods.

iv. The ITTC-57/78 method should be used to extrapolate the model-scale results to the full-scale HSMV.

v. The trim, pitch and heave response of the converted vessel should be computed to confirm its longitudinal stability.

vi. An experimental investigation should be carried out to verify the predicted performance before practical implementation.

ACKNOWLEDGMENTS

The authors acknowledge the Tertiary Education Trust Fund (TETFund) of Nigeria for funding this research, and the management of the Federal University of Technology Ikot Abasi and Akwa Ibom State University, Ikot Akpaden, for providing an enabling environment for the research.

REFERENCES

[1] Aghaei Pour, P., Hakanen, J., & Miettinen, K. (2024). A surrogate-assisted a priori multiobjective evolutionary algorithm for constrained multiobjective optimization problems. *Journal of Global Optimization, 90*(2), 459–485.

[2] Ayob, A. F. M., Ray, T., & Smith, W. F. (2011). Scenario-based hydrodynamic design optimization of high-speed planing craft for coastal surveillance. In *2011 IEEE Congress of Evolutionary Computation (CEC)*. IEEE.

[3] Ayob, A. F. M., Ray, T., & Smith, W. F. (2012). A hydrodynamic preliminary design optimization framework for high speed planing craft. *Journal of Ship Research, 56*(1), 35–47.

[4] Collu, M., Patel, M. H., & Trarieux, F. (2007, June 28–30). *A unified mathematical model for high speed hybrid (air and water-borne) vehicles* [Paper presentation]. 2nd International Conference on Marine Research and Transportation (ICMRT), Ischia, Naples, Italy.

[5] Collu, M., Patel, M. H., & Trarieux, F. (2010). The longitudinal static stability of an aerodynamically alleviated marine vehicle, a mathematical model. *Proceedings of the Royal Society A: Mathematical, Physical and Engineering Sciences, 466*(2116), 1055–1075.

[6] Collu, M., Williams, A. W. G., Patel, M. H., & Trarieux, F. (2009). Aerodynamically alleviated marine vehicles (AAMV): Development of a mathematical framework to design high speed marine vehicles with aerodynamic surfaces. In *Proceedings of the International Conference on High Performance Marine Vehicles (HPMV09)*, Shanghai, China.

[7] Costa, L., & Oliveira, P. (2003). An elitist genetic algorithm for multiobjective optimization. In M. G. C. Resende & J. P. de Sousa (Eds.), *Metaheuristics: Computer decision-making* (pp. 217–236). Springer.

[8] Day, A. H., & Doctors, L. J. (1996). Minimal-resistance hullforms for high-speed craft. *Transactions of the Royal Institution of Naval Architects, 138*, 194–210.

[9] Deb, K., Pratap, A., Agarwal, S., & Meyarivan, T. (2002). A fast and elitist multiobjective genetic algorithm: NSGA-II. *IEEE Transactions on Evolutionary Computation, 6*(2), 182–197. https://doi.org/10.1109/4235.996017

[10] Faltinsen, O. M. (2006). *Hydrodynamics of high-speed marine vehicles*. Cambridge University Press.

[11] Fiala, V., Dvořák, P., & Pechánek, R. (2022). Practical approach to multi-objective optimization in ANSYS software. In *2022 20th International Conference on Mechatronics – Mechatronika (ME)* (pp. 1–6). IEEE.

[12] Giraldo-Pérez, E., Betancur, E., & Osorio-Gómez, G. (2022). Experimental and statistical analysis of the hydrodynamic performance of planing boats: A comparative study. *Ocean Engineering, 262*, Article 112227.

[13] Huang, F., Wang, L., & Yang, C. (2015). Hull form optimization for reduced drag and improved seakeeping using a surrogate-based method. In *Proceedings of the 25th International Ocean and Polar Engineering Conference (ISOPE 2015)*, Kona, Hawaii, USA. International Society of Offshore and Polar Engineers.

[14] Isaacs, A., Ray, T., & Smith, W. (2007). An evolutionary algorithm with spatially distributed surrogates for multiobjective optimization. In *Progress in artificial life (ACAL 2007)* (Lecture Notes in Computer Science, Vol. 4828). Springer.

[15] Jahanbakhsh, E., Panahi, R., & Seif, M. S. (2008). Development of a numerical tool for hydrodynamic simulation of high-speed planing craft. In *Proceedings of the 6th International Conference on High-Performance Marine Vehicles (HIPER 2008)* (pp. 311–316).

[16] James, D., & Collu, M. (2015). Aerodynamically alleviated marine vehicle (AAMV): Bridging the maritime-to-air domain. In *Proceedings of the 13th International Conference on Fast Sea Transportation (FAST 2015)*. Society of Naval Architects and Marine Engineers.

[17] Jin, Y., & Sendhoff, B. (2008). *Methods for multi-objective optimization using evolutionary algorithms* (U.S. Patent No. 7,363,280). U.S. Patent and Trademark Office.

[18] Jose, S., & Vijayalakshmi, C. (2020). Optimization of multi-objective problem using evolutionary algorithms. *International Journal of Scientific & Technology Research, 9*(4).

[19] Kim, K. J. (1989). *Ship flow calculations and resistance minimization* [Doctoral dissertation, Chalmers University of Technology].

[20] Matveev, K. I., & Dubrovsky, V. A. (2007). Aerodynamic characteristics of a hybrid trimaran model. *Ocean Engineering, 34*(3), 616–620.

[21] Mohamad Ayob, A. F., Ray, T., & Smith, W. F. (2009). An optimization framework for the design of planing craft. In *International Conference on Computer Applications in Shipbuilding (ICCAS 2009)*. Royal Institution of Naval Architects.

[22] Molland, A. F., Turnock, S. R., & Hudson, D. A. (2011). *Ship resistance and propulsion: Practical estimation of ship propulsive power*. Cambridge University Press.

(This work is licensed under a Creative Commons Attribution 4.0 International License.)

International Journal of Engineering Research & Technology (IJERT)
ISSN: 2278-0181
Vol. 15 Issue 11 , November - 2026

[23] Ni, Q., Ji, S., Jiang, Y., Li, S., Liu, Y., & Xu, W. (2023). Numerical study on the aerodynamic and hydrodynamic performances of an ultra-high-speed AAMV. *Journal of Hydrodynamics, 35*(5), 980–992.
[24] Ohwofadjeke, P., Udo, A., & Jonah, J. (2024). Characterisation of fluid-structure interaction on hydrodynamic performance of different ship hulls using ANSYS. *Computational Engineering and Physical Modelling, 7*(1), 12–32.
[25] Pacuraru, F., Mandru, A., & Bekhit, A. (2022). CFD study on hydrodynamic performances of a planing hull. *Journal of Marine Science and Engineering, 10*(10), Article 1523. https://doi.org/10.3390/jmse10101523
[26] Samaei, S. R., & Asadian, G. M. (2025). Parameter study for enhancing the speed of a high-speed craft prototype with adequate manoeuvrability. *International Journal of Maritime Technology*, 28–43.
[27] Song, Y., Du, X., & Hu, Y. (2024). Numerical study of the ultra-high-speed aerodynamically alleviated marine vehicle motion stability in winds and waves. *Journal of Marine Science and Engineering, 12*(7), Article 1229. https://doi.org/10.3390/jmse12071229
[28] Song, Y., Du, X., Jiang, Y., & Hu, Y. (2023). Numerical investigation on the resistance characteristics and motion characteristics of the ultra-high-speed aerodynamically alleviated marine vehicle in regular head waves. *Ocean Engineering, 289*, Article 116284.
[29] Song, Y., Du, X., Jiang, Y., & Hu, Y. (2024). Experimental investigation on the longitudinal stability of the aerodynamically alleviated marine vehicle with multi-steps. *Physics of Fluids, 36*(10).
[30] Tavakoli, S., Zhang, M., Kondratenko, A. A., & Hirdaris, S. (2024). A review on the hydrodynamics of planing hulls. *Ocean Engineering, 303*, Article 117046.
[31] Yun, L., Bliault, A., & Rong, H. Z. (2018). *High speed catamarans and multihulls: Technology, performance, and applications*. Springer.
[32] Zhang, B. J., & Zhang, Z. X. (2015). Research on theoretical optimization and experimental verification of minimum resistance hull form based on Rankine source method. *International Journal of Naval Architecture and Ocean Engineering, 7*(5), 785–794.
[33] Zhang, S., Zhang, B., Tezdogan, T., Xu, L., & Lai, Y. (2018). Computational fluid dynamics-based hull form optimization using approximation method. *Engineering Applications of Computational Fluid Mechanics, 12*(1), 74–88.

(This work is licensed under a Creative Commons Attribution 4.0 International License.)